

**SER Compliance with  
WCAP-12610-P-A & CENPD-404-P-A Addendum 1-A  
“Optimized ZIRLO™” (Non-Proprietary)**

February 2008

Westinghouse Electric Company  
P.O. Box 355  
Pittsburgh, Pennsylvania 15230-0355

©2008 Westinghouse Electric Company LLC  
All Rights Reserved

## 1.0 Introduction

This report is being provided to address Conditions 6 and 7 of Section 5.0 of the SER to topical report WCAP-12610-P-A & CENPD-404-P-A Addendum 1-A (Reference 1) to provide Optimized ZIRLO™\* LTA and creep/growth data. The data demonstrate that the current fuel performance models are applicable for Optimized ZIRLO™ fuel rods.

Condition 6 of the SER to Reference 1 states the following:

6. “The licensee is required to ensure that Westinghouse has fulfilled the following commitment: Westinghouse shall provide the NRC staff with a letter(s) containing the following information (Based on the schedule described in response to RAI #3):
  - a. Optimized ZIRLO™ LTA data from Byron, Calvert Cliffs, Catawba, and Millstone.
    - i. Visual
    - ii. Oxidation of fuel rods
    - iii. Profilometry
    - iv. Fuel rod length
    - v. Fuel assembly length
  - b. Using the standard and Optimized ZIRLO™ database including the most recent LTA data, confirm applicability with currently approved fuel performance models(e.g., measured vs. predicted).

Confirmation of the approved models’ applicability up through the projected end of cycle burnup for the Optimized ZIRLO™ fuel rods must be completed prior to their initial batch loading and prior to the startup of subsequent cycles. For example, prior to the first batch application of Optimized ZIRLO™, sufficient LTA data may only be available to confirm the models’ applicability up through 45 GWd/MTU. In this example, the licensee would need to confirm the models up through the end of the initial cycle. Subsequently, the licensee would need to confirm the models, based upon the latest LTA data, prior to re-inserting the Optimized ZIRLO™ fuel rods in future cycles. Based upon the LTA schedule, it is expected that this issue may only be applicable to the first few batch implementations since sufficient LTA data up through the burnup limit should be available within a few years.”

Condition 7 of the SER to Reference 1 states the following:

7. “The licensee is required to ensure that Westinghouse has fulfilled the following commitment: Westinghouse shall provide the NRC staff with a letter containing the following information (Based on the schedule described in response to RAI #11):
  - a. Vogtle growth and creep data summary reports.
  - b. Using the standard ZIRLO™ and Optimized ZIRLO™ database including the most recent Vogtle data, confirm applicability with currently approved fuel performance models (e.g., level of conservatism in W rod pressure analysis, measured vs. predicted, predicted minus measured vs. tensile and compressive stress).

---

\* ZIRLO™ trademark property of Westinghouse Electric Company LLC

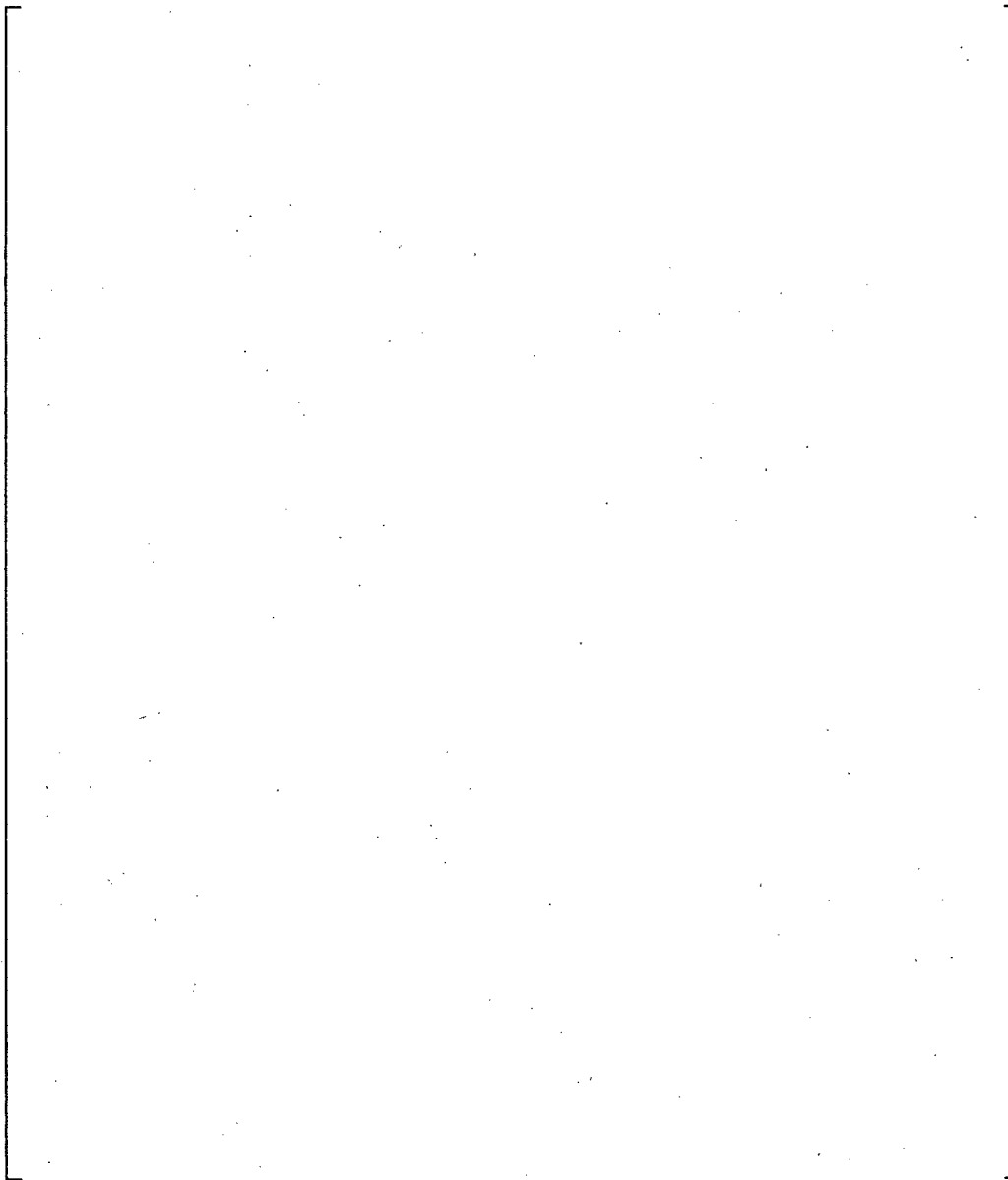
Confirmation of the approved models' applicability up through the projected end of cycle burnup for the Optimized ZIRLO™ fuel rods must be completed prior to their initial batch loading and prior to the startup of subsequent cycles. For example, prior to the first batch application of Optimized ZIRLO™, sufficient LTA data may only be available to confirm the models' applicability up through 45 GWd/MTU. In this example, the licensee would need to confirm the models up through the end of the initial cycle. Subsequently, the licensee would need to confirm the models, based upon the latest LTA data, prior to re-inserting the Optimized ZIRLO™ fuel rods in future cycles. Based upon the LTA schedule, it is expected that this issue may only be applicable to the first few batch implementations since sufficient LTA data up through the burnup limit should be available within a few years."

**2.0 Condition 6 Compliance – LTA Data**

**2.1 LTA Program Schedule**

The four listed LTA programs are at different stages of their execution. While the Byron LTA program has concluded, the Calvert-Cliffs, Catawba and Millstone LTA programs are still on-going. The Byron LTA program included both stress relief annealed (SRA) and partially recrystallized annealed (PRXA) Optimized ZIRLO™ while the other three LTA programs only included PRXA Optimized ZIRLO™. Table 1 summarizes the status of the various LTA programs. It should be noted that the availability of data and plans associated with future dates are projections and depend on the operation of the plants and thus may change in the future.

Table 1 – Optimized ZIRLO™ LTA Irradiation and Planned Examination Status



a,c

## 2.2 Data Presentation and Analysis

### 2.2.1 Visual Examination

Visual inspections were performed subsequent to each irradiation cycle in all of the LTA programs. A summary of the visual inspections from each of the on-going LTA programs is described in the following subsections. In summary, no anomalous performance was observed.

#### Byron LTA

Visual inspections were performed on the Byron LTAs after each of the three irradiation cycles. Minor crud was reported on both SRA Optimized ZIRLO™ and Standard ZIRLO™ fuel rods at each inspection. No anomalies were reported for any of the three alloys.

#### Calvert Cliffs LTA

Visual inspections were performed on assemblies [ ]<sup>a,c</sup> after one 24-month cycle. Minor crud was observed on fuel rods in both assemblies but no anomalies were found. There were no areas of localized crud or corrosion accumulation.

#### Catawba 1 LTA

The Catawba LTA program is composed of [ ]<sup>a,c</sup> assemblies of the Westinghouse 17x17 Next Generation Fuel (NGF) design. [ ]<sup>a,c</sup> LTAs were inspected after 1 cycle of operation in the Catawba Unit 1 plant. Dark crud was observed on the fuel rods and on many assembly components. The dark crud is thought to be due to the replacement of steam generators, consistent with the crud observed in the McGuire plants following steam generator replacement there. [ ]<sup>a,c</sup> LTAs were inspected after 2 cycles of operation in the Catawba Unit 1 plant. Minor quantity of crud was observed on the fuel rods in the assemblies but no anomalies were observed.

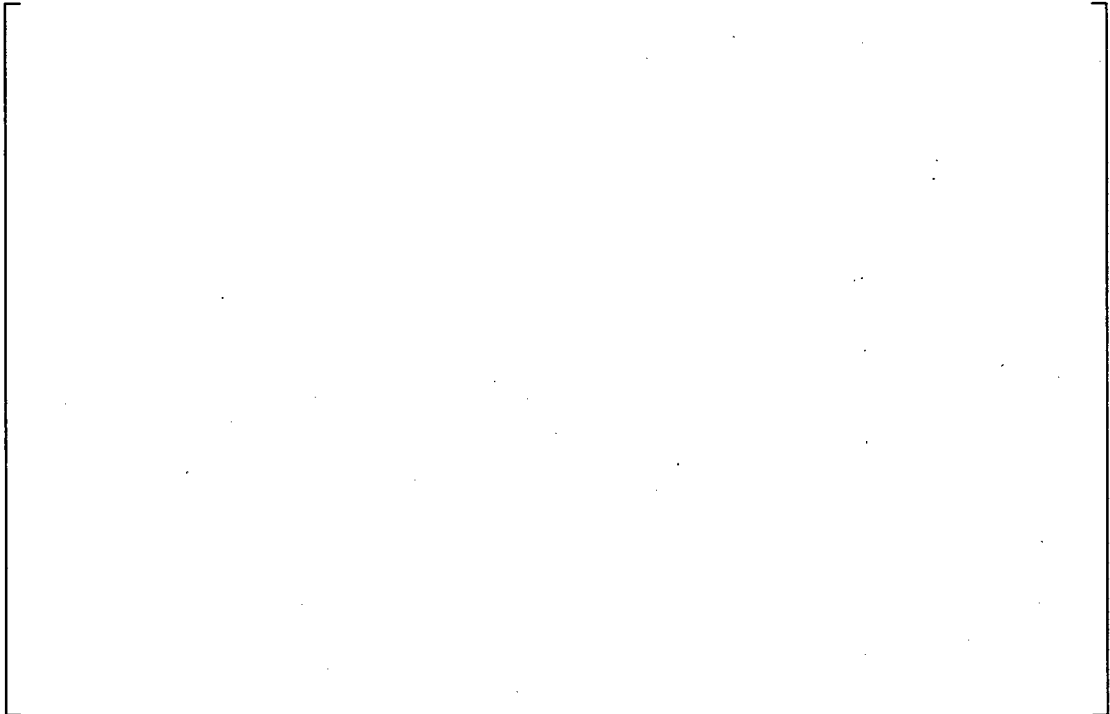
#### Millstone 3 LTA

The Millstone LTA program is composed of [ ]<sup>a,c</sup> assemblies of the Westinghouse 17x17 NGF design. [ ]<sup>a,c</sup> LTAs were inspected after 1 cycle of operation. Minor crud was observed on fuel rods in both the NGF LTAs and Standard ZIRLO™ Robust Fuel Assembly (RFA) assemblies. No anomalies were observed. [ ]<sup>a,c</sup> NGF LTAs were inspected after 2 cycles of operation in the Millstone Unit 3 plant. Expected normal quantity of non-adherent crud was observed on the fuel rods in the assemblies but no anomalies were observed.

### 2.2.2 Oxidation of Fuel Rods

Fuel rod oxide measurements are currently available from the Byron, Catawba, and Millstone LTAs. In the future, per the schedule shown in Table 1, additional data are expected to become available from the continuation of the Catawba, Millstone, and Calvert Cliffs LTA programs. The oxide thickness from the Byron LTA program was measured after each cycle of operation. The oxide thickness from the Catawba and Millstone LTA programs was measured after 2 cycles of operation. The data (Figures 1 and 2) show the corrosion rate of the Optimized ZIRLO™ to be about 30% lower relative to that of the Standard ZIRLO™.

Since the oxidation of Optimized ZIRLO™ is well below the ZIRLO™ values and the corrosion calculations are based on the ZIRLO™ model, corrosion calculations remain valid and the Optimized ZIRLO™ rods will operate within the design criteria for the projected operation.



a,b,c

Figure 1 – Measured Oxide Thickness Plotted as a Function of the Modified Fuel Duty Index



a,b,c

Figure 2 – Measured Oxide Thickness Plotted as a Function of Rod Peak Burn-up

2.2.3 Profilometry

The fuel rod profile was measured after one cycle of operation on [ ]<sup>a,c</sup> PRXA Optimized ZIRLO™ rods [ ]<sup>a,c</sup>. These rods were inserted into the Byron [ ]<sup>a,c</sup> host assembly prior to the third cycle of irradiation of the host assembly. [ ]

[ ]<sup>a,c</sup>. Measured versus predicted calculations were performed using the PAD 4.0 fuel rod performance code. The measured minus best-estimate-PAD 4.0-predicted results for Byron are presented in Figure 3. For the diameter profile measurements after one irradiation cycle and prior to clad-pellet contact, 95% of the rods [ ]<sup>a,c</sup> are within the average measured minus predicted PAD 4.0 creep model upper bound (UB) and lower bound (LB) limits. The remaining 5% of the rods [ ]<sup>a,c</sup> is above the average UB creep, indicating that PAD over-predicted the creep relative to the measured creep for [ ]<sup>a,c</sup>. Experience has shown that later clad creep down to gap closure relative to the predicted burnup has little effect on internal pressure and the fuel rod peak thermal condition. Maximum pressure occurs well after gap closure so maximum pressure is not affected. Representative measured vs. PAD predictions for the PRXA Optimized ZIRLO™ fuel rods are shown in Figures 4 to 6.



Figure 3 - Measured minus best-estimate-PAD-predicted Byron data.



Figure 4 – Comparison of Fuel Rod Diameter between Measured and PAD 4.0 Predicted for PRXA Optimized ZIRLO™ Rod A06 irradiated in Byron.



Figure 5 - Comparison of Fuel Rod Diameter between Measured and PAD 4.0 Predicted for PRXA Optimized ZIRLO™ Rod B07 irradiated in Byron.



Figure 6 - Comparison of Fuel Rod Diameter between Measured and PAD 4.0 Predicted for PRXA Optimized ZIRLO™ Rod C16 irradiated in Byron.

Figures 4 to 6 show good agreement in the outer diameter profiles between the PAD code predictions and the measured values. In particular, the region of highest creep rate (i.e., elevations of 80 to 120 inches) shows excellent agreement. The predictions follow the measured axial shape which indicates that the code is well-behaved with respect to the in-reactor irradiation creep model temperature dependence. The diameter profile measurements after one irradiation cycle and prior to clad-pellet contact are within the PAD 4.0 creep model upper bound (UB) and lower bound (LB) limits for [

] <sup>a,c</sup> are above the LB creep, indicating that the PAD predicted creep was greater than the measured creep for [ ] <sup>a,c</sup>. As stated above, experience has shown that slower clad creep down to gap closure has little effect on internal pressure and the fuel rod peak thermal condition. These comparisons demonstrate that the creep rate of the PRXA Optimized ZIRLO™ is equivalent to that of the Standard ZIRLO™ and confirms that the licensed PAD 4.0 creep model is applicable for Optimized ZIRLO™. Similarly, the FATES code would also be applicable in predicting creep behavior of the PRXA Optimized ZIRLO™ in the CE fuel design, since it uses the same creep model as PAD.

The PAD 4.0 prediction is best in the region of the rod that is limiting for No Clad Lift-Off (NCLLO) from 90 to 120 inches. Therefore, the current NCLLO calculations remain valid. This is also the region of the rod that would be limiting for creep collapse. Since the creep model predictions are within uncertainty limits in this region, creep collapse calculations remain valid.

#### 2.2.4 Fuel Rod Length

Fuel rod length was measured on the Byron SRA Optimized ZIRLO™ fuel rods and the Byron, Catawba, and Millstone PRXA Optimized ZIRLO™ fuel rods. The measured fuel rod length is plotted with the Standard ZIRLO™ assembly average fuel rod growth database in Figure 7. The measurements show the growth of SRA and PRXA Optimized ZIRLO™ to be within the scatter band of the ZIRLO™ fuel rod growth database.



Figure 7 – Fuel Rod Growth Measurements from SRA and PRXA Optimized ZIRLO™

Shown in Figure 7 is the upper growth line used in shoulder gap calculations and the lower growth line used for rod internal pressure (RIP) uncertainty calculations in PAD 4.0. Based on the trends observed in the Optimized ZIRLO™ fuel rod growth the design analyses for the shoulder gap closure and for the RIP calculations remain valid. In the post irradiation exams for fuel rod growth, no significant increase in shoulder gap has been observed. The trend is that the shoulder gap decreases with burnup. Therefore, the design evaluations for fuel rod to spacer grid engagement remain valid.

### 2.2.5 Fuel Assembly Length

Fuel assembly growth data are currently available from the Byron, Catawba, and Millstone programs. The assembly growths of the Optimized ZIRLO™ LTAs are plotted in Figure 8 along with the Standard ZIRLO™ database. The comparison shows Optimized ZIRLO™ to behave comparable to Standard ZIRLO™.



Figure 8 – Assembly Growth Plotted as a Function of Fast Neutron Fluence

The fuel assembly growth trends are design specific. In Figure 9 the fuel assembly growth data for the 17x17 standard assembly designs is plotted along with the NGF LTA data and the upper bound, best estimate and lower bound growth curves. It can be observed in Figure 9 that the Optimized ZIRLO™ NGF LTA growth data is within the growth bounds. Therefore the design calculations for fuel assembly growth remain valid.



Figure 9 – 17x17 Standard Assembly Growth Plotted as a Function of Burnup

### 2.3 Summary

The LTA measurements showed the corrosion rate of the SRA Optimized ZIRLO™ and PRXA Optimized ZIRLO™ to be significantly lower than that of the Standard ZIRLO™ and thus this property is bounded by the predictive capability of the approved ZIRLO™ corrosion model. The measured Byron fuel rod creep data confirm that the creep rate of the PRXA Optimized ZIRLO™ is in agreement with the licensed creep model. Similarly, the measured SRA/PRXA Optimized ZIRLO™ fuel rod growth is also within the predictive capability of the Standard ZIRLO™ fuel rod growth model as the measured values are well within the scatter band of the Standard ZIRLO™ fuel rod growth database. The measured Optimized ZIRLO™ fuel assembly growth is also within the scatter band of the Standard ZIRLO™ fuel assembly growth database.

Based on these measurements and evaluations, the fuel rod and fuel assembly design calculations remain valid and the Optimized ZIRLO™ fuel will operate within design criteria.

**3.0 Condition 7 Compliance – Creep/Growth Data**

**3.1 Creep/Growth Test Program Schedule and Status**

The irradiation schedule of the Creep/Growth test is shown in Figure 10. The current status is as follows. Test assemblies A1, A3 and A5 have been discharged. Table 2 lists the status of the data evaluation. The data evaluation consists of sample laser outside diameter (OD) and length measurements, sample oxide thickness measurements, coolant temperature calculations based on the post-run fuel assembly powers, determination of the gamma-heating rate, sample temperature and hoop stress, and measurement of the fast fluence by retrospective dosimetry. In the case of test assemblies A1, A5, and A3, the OD, length and oxide thickness measurements have been performed and the OD and length strains calculated. The coolant temperature, sample temperature and hoop stress analysis are completed. The fluence/dosimetry measurements for test assembly A1 are completed and evaluation of the data is in-progress. In the interim, calculated fluence values are being used.

The irradiation of test assembly A2 has been completed and it is currently in temporary storage in the Vogtle fuel pool. Test assembly A2 is scheduled for shipment to a hot cell in January 2009.

Test assembly A4 is still under irradiation. The test assemblies A1, A5, and A3 data are available for evaluation. Data from the remaining test assemblies will be provided in the future.

Table 2 – Status of the Creep/Growth Data Evaluation

Assembly	Parameter	Status
A1, A3, A5	OD	Complete
A1, A3, A5	Length	Complete
A1, A3, A5	Oxide thickness	Complete
A1, A3, A5	Coolant T	Complete
A1, A3, A5	Hoop Stress & T	Complete
A1, A3, A5	Fluence	Calculations are available. Measurements for A1 are available and evaluation is in-progress
Notes:		
1. A2 is in temporary storage in the Vogtle fuel pool		
2. A4 is in-reactor		

Cycle#:	10	11	12	13	14	15
Date:	Fall 2002	Spring 2004	Fall 2005	Spring 2007	Fall 2008	Spring 2010
<u>Assembly</u>	A1, A2, and A3 contain [					] <sup>a,c</sup>
A1	x-----x					
A2	x-----x					
A3	x-----x					
	A4 and A5 contain [					] <sup>a,c</sup>
A4		x-----x				
A5		x-----x				

Figure 10 – Irradiation Schedule of the Creep/Growth Test

### 3.2 Creep/Growth Irradiation Conditions

The samples are located in segmented rods suspended inside the fuel assembly thimble tubes. All of the test samples are placed in positions approximately 90 cm above and below the core midplane. The samples are free-standing in the core. That is, the samples are not located at the axial positions of the mid-grids or intermediate flow mixer (IFM) grids. The samples are radially located relatively close to core center. The samples are always hosted by a one-cycle burned fuel assembly. Fast flux calculations showed that the fast flux for these conditions is approximately the same for all of the samples (the fast flux is approximately constant) and remains the same from cycle-to-cycle. The dosimetry measurements are being performed to confirm these calculations.

The amount of gamma-heating was determined by testing samples having the same tubing with two different internal heating rates. The samples did not contain any fuel. Each sample had either a solid cylinder or an internal tube to support the sample if collapse were to occur (the samples were tested at compressive stress levels that calculations showed would not result in collapse). Since the mass of the solid cylinders was much greater than the internal tubes, these two different types of samples generated different amounts of internal heat due to gamma-heating. As a result, the gamma-heating was evaluated by parametric calculations using the diameter strain data. The gamma-heat was used to calculate the sample temperature distributions. The calculated temperatures for test assemblies A1, A5, and A3 were in the range of [ ]<sup>a,c</sup>. The samples in the lowest axial positions are associated with temperatures of [ ]<sup>a,c</sup>, and the samples in the highest axial position are associated with temperatures of [ ]<sup>a,c</sup>.

### 3.3 Creep/Growth Test Data

The results to be presented are 1) the irradiation growth and creep of Standard ZIRLO™ and PRXA Optimized ZIRLO™ and 2) the irradiation creep of Standard ZIRLO™ under tension and compression hoop stresses. The presentation of the irradiation growth and irradiation creep data summarizes currently available Creep/Growth data in partial compliance with Condition 7a of the SER to Reference 1.

The measurement accuracy associated with the OD and length laser measurements is excellent. Consider the OD data. The 95% confidence interval of the mean OD value is about [ ]<sup>a,c</sup>. The 95% confidence interval measurement error is very small because the data for each sample consist of [ ]<sup>a,b,c</sup>.

The fast fluence for test assemblies A1, A5, and A3 are [ ]<sup>a,c</sup> respectively. The Creep/Growth test does not contain fuel so the irradiation is properly characterized by fast fluence and not burnup.

#### 3.3.1 Irradiation Growth

Figures 11 and 12 present the diameter irradiation growth data for Standard ZIRLO™, PRXA Optimized ZIRLO™ and SRA Optimized ZIRLO™ fabricated by a [ ]<sup>a,c</sup> 4-pass tube reduction sequence from TREX to final size tubing. The irradiation growth samples had holes to allow the coolant water to be both at the OD and ID. This insured that the samples were unstressed. Each marker in Figures 11 and 12 represents one sample. The strain scale was selected to present the 1- and 2-cycle data using the same range. Irradiation growth data are available for two PRXA Optimized ZIRLO™ lots. Figures 11 and 12 show that the irradiation growth of the two PRXA Optimized ZIRLO™ lots is consistent. Further, the irradiation growth of PRXA Optimized ZIRLO™ and Standard ZIRLO™ is comparable.

ZIRLO Diameter Irradiation Growth  
Vogtle 2 Cycle 10 (Samples open to coolant water), 305-315 C

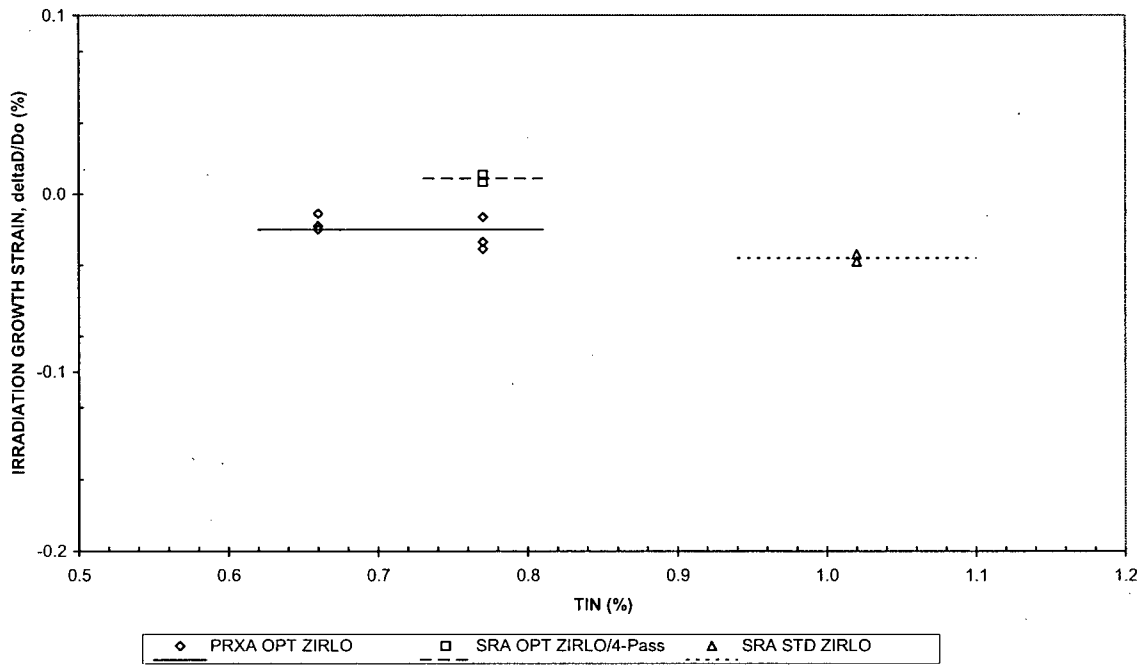


Figure 11 – ZIRLO™ Irradiation Growth after 1 Cycle (Test Assembly A1)



a,b,c

Figure 12 – ZIRLO™ Irradiation Growth after 2 Cycles (Test Assembly A3)

3.3.2 Irradiation Creep

The irradiation creep was measured using samples filled with helium gas. The internal gas pressure was either below or above system pressure so that the samples were in either compression or tension hoop stress, respectively. The irradiation creep diameter strain,  $\Delta D/D_o(ic)$ , was calculated from the total measured strain,  $\Delta D/D_o(total)$ , and the average irradiation growth strain,  $\Delta D/D_o(ig)$ , according to,

$$\Delta D/D_o(ic) = \Delta D/D_o(total) - \Delta D/D_o(ig)$$

Figures 13 and 14 presents the diameter irradiation creep data for Standard ZIRLO™, PRXA Optimized ZIRLO™ (tube samples from two lots) and SRA Optimized ZIRLO™ tubes fabricated by a ]<sup>a,c</sup> 4-pass tube reduction sequence from TREX to final size tubing. Each marker in Figures 13 and 14 represents one sample. The strain scale was selected to present the 1- and 2-cycle data using the same range. The irradiation creep of all of the materials is comparable. This shows that 1) the irradiation creep of PRXA Optimized ZIRLO™ and Standard ZIRLO™ are comparable, and 2) Optimized ZIRLO™ with the same irradiation creep may be fabricated with either a PRXA or SRA final microstructure by changing the tube reduction process. Comparison of Figures 13 and 14 with Figures 11 and 12 (note the difference in the strain scales between Figures 13 and 14 versus Figures 11 and 12) shows that the irradiation growth of PRXA Optimized ZIRLO™ and Standard ZIRLO™ is more than an order of magnitude less than the irradiation creep.

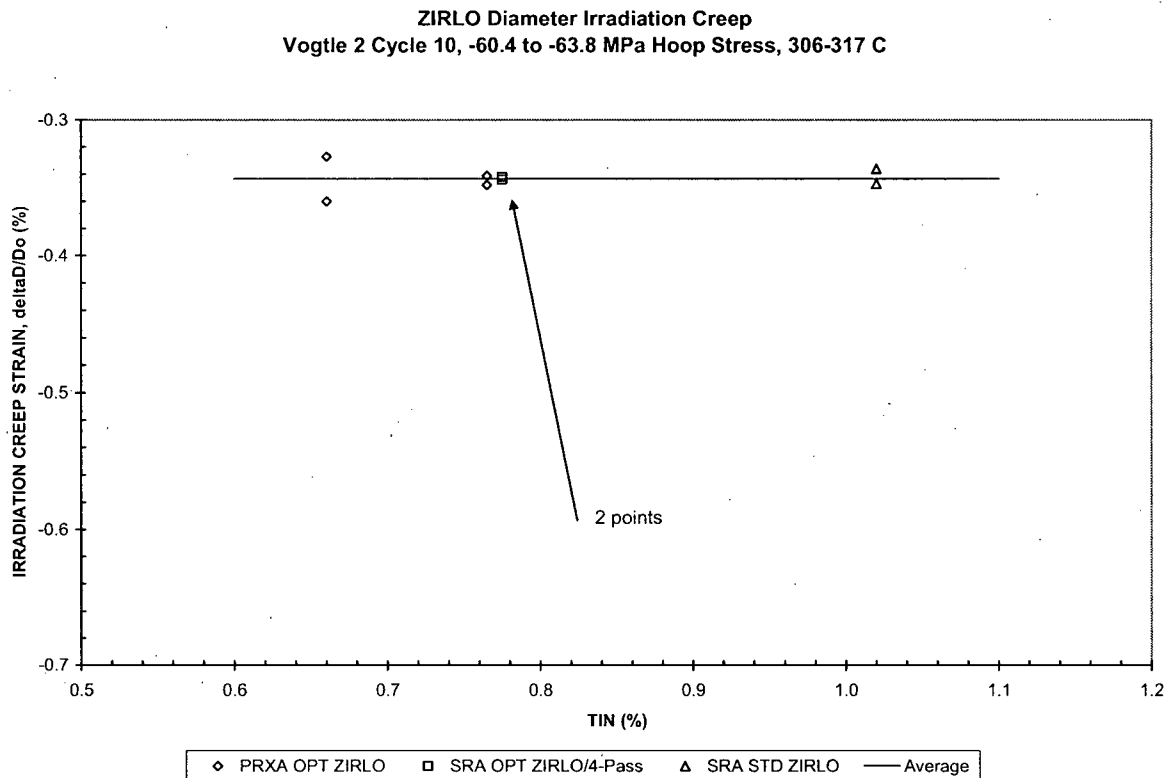


Figure 13 – ZIRLO™ Irradiation Creep after 1 Cycle (Test Assembly A1)



Figure 14 – ZIRLO™ Irradiation Creep after 2 Cycles (Test Assembly A3)

Figures 15 to 17 present the irradiation creep data for Standard ZIRLO™ for tension and compression hoop stresses. The stress ranges are from about [ ]<sup>a,b,c</sup> hoop stress. This hoop stress range approximately envelopes the range of hoop stresses experienced by fuel rods during normal operation. Each marker in Figures 15 to 17 represents one sample. In the case of test assembly A1, compression hoop stress data are available for [ ]<sup>a,b,c</sup> and tension hoop stress data are available for [ ]<sup>a,b,c</sup>. In the case of test assembly A5, compression hoop stress data are available for [ ]<sup>a,b,c</sup> and tension hoop stress data are available for [ ]<sup>a,b,c</sup>. In the case of test assembly A3, compression hoop stress data are available for [ ]<sup>a,b,c</sup> and tension hoop stress data are available for [ ]<sup>a,b,c</sup>. Most of the stress levels include duplicate samples to confirm strain level consistency. Figures 15 to 17 show that the scatter of duplicate samples is negligible. Further, Figures 15 to 17 show that the data are very consistent between stress levels, and that the behavior is linear as a function of hoop stress. The non-zero  $\Delta D/D_0$  intercept at zero stress is attributed to the effect of internal stresses as discussed in Reference 2.



Figure 15 – Irradiation Creep in Tension and Compression after 1 Cycle (Test Assembly A1)



Figure 16 – Irradiation Creep in Tension and Compression after 1 Cycle (Test Assembly A5)

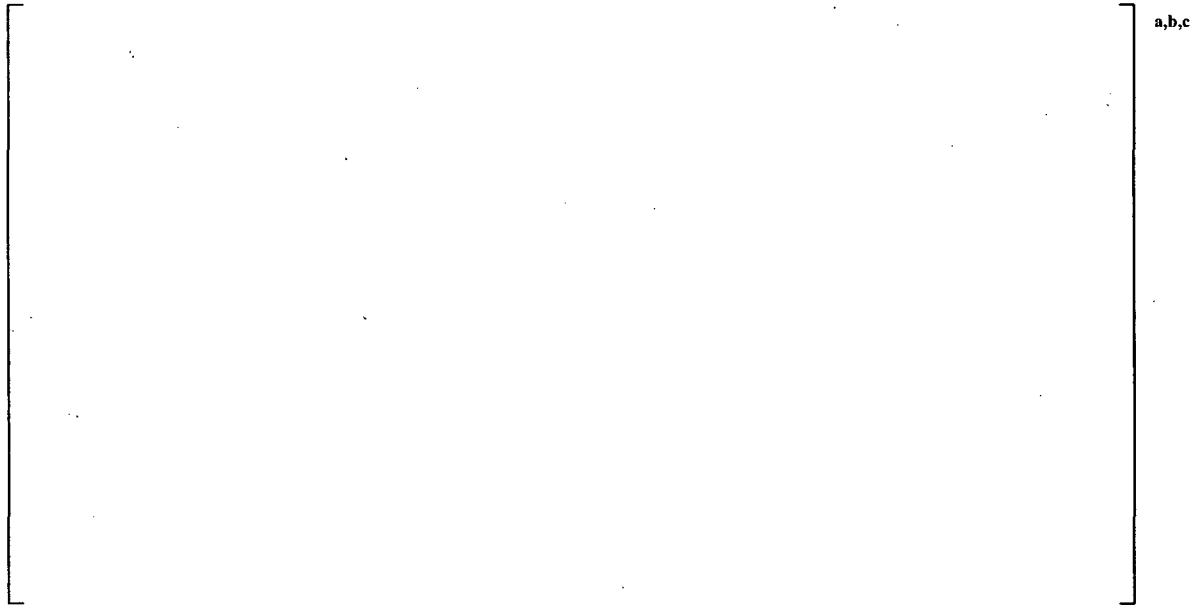


Figure 17 – Irradiation Creep in Tension and Compression after 2 Cycles (Test Assembly A3)

### 3.4 Discussion of the OD Strain Components

Figures 15 to 17 present the Standard ZIRLO™ irradiation creep strain for compressive and tensile hoop stresses. The currently available Creep/Growth data are not sufficient to separate the total strain into transient and steady state components. However, Halden measurements on Standard ZIRLO™ samples are available (Tests IFA-663 and IFA-617) that allow the separation of the total strain into transient and steady state components. The duration of the transient component is,

298 FPH at a flux of  $2.7 \times 10^{13}$  n/cm<sup>2</sup>-s (E>1) for Halden Test IFA-663, and  
 243 FPH at a flux of  $4.5 \times 10^{13}$  n/cm<sup>2</sup>-s (E>1) for Halden Test IFA-617.

In terms of fluence, the average duration of the transient is,

$$\begin{aligned} 2.7 \times 10^{13} \text{ n/cm}^2\text{-s} * 298 \text{ h} * 3600 \text{ s/h} &= 0.029 \times 10^{21} \text{ n/cm}^2 \\ 4.5 \times 10^{13} \text{ n/cm}^2\text{-s} * 243 \text{ h} * 3600 \text{ s/h} &= 0.039 \times 10^{21} \text{ n/cm}^2 \\ &\underline{0.034 \times 10^{21} \text{ n/cm}^2 \text{ average}} \end{aligned}$$

The fluence for the Creep/Growth test assemblies are [

] <sup>a,c</sup>.

Based on the Halden data, the test assembly samples are in steady state creep for [ ] <sup>a,c</sup> of their irradiation period. Therefore, a significant fraction of the total irradiation creep strains presented in Figures 15 to 17 is steady state irradiation creep.

According to the original reported evaluation of Halden test IFA-585 (Reference 3), the steady state irradiation creep rate in tension is 50% higher than in compression. The original evaluation has been updated (Reference 4). Reference 4 showed that the Halden test is most likely in transient and not in steady state irradiation creep. Hence, firm conclusions cannot be reached on the behavior of steady state irradiation creep with the Halden IFA-585 test. Further, note that these results were based on testing with fully recrystallized Zr-2.

The total diameter irradiation creep strain,  $\Delta D/D_0$ , is the sum of two terms. The first term is a transient component and the second term is a steady state component. According to the Halden data presented above, the transient component is saturated once the fluence reaches  $3.4 \times 10^{19} \text{ n/cm}^2 E > 1$ . Hence, for all fluence increases above  $3.4 \times 10^{19} \text{ n/cm}^2 E > 1$ , the incremental irradiation creep strain is from the steady state component. If the Standard ZIRLO™ steady state irradiation creep rate in tension was significantly greater than in compression, then the compression and tension irradiation creep data shown in Figures 15 to 17 could not be described by one linear equation because [ ]<sup>a,c</sup> of the test assembly irradiation periods are in steady state creep. Instead, the data would have to be described by two linear equations, one in the compression stress range and the second with a higher slope in the tension stress range. Since the Creep/Growth compression and tension hoop stress data are described by one linear equation and not two, the steady state irradiation creep is the same in tension and compression for the Standard ZIRLO™ and Optimized ZIRLO™ fuel cladding produced according to Westinghouse processes.

### 3.5 Fuel Performance Models

The purpose of the Vogtle Creep/Growth tests was to confirm that irradiation creep is the same for ZIRLO™ and Optimized ZIRLO™, and that the steady state irradiation creep rate is the same in tension and compression. This was accomplished in a carefully controlled test using prepressurized tubing samples without fuel. The conclusions are drawn based on the relative performance of the test samples under carefully controlled conditions. The design fuel rod performance methods cannot be directly applied to predict the creep performance of these test samples. A finite element modeling approach is being investigated to model the tubing samples and develop creep predictions for the samples using the ZIRLO™ creep model from PAD. However, the results are sensitive to modeling assumptions regarding the geometry and loading condition (e.g., pressure, temperature and flux) of the short samples, and this effort continues as a work in progress.

The PAD 4.0 irradiation growth and irradiation creep models were benchmarked using Standard ZIRLO™. The FATES code uses the same creep model as PAD. The Creep/Growth data presented above confirm that irradiation growth and irradiation creep are comparable for Standard ZIRLO™ and PRXA Optimized ZIRLO™. This meets Condition 7b of the SER to Reference I.

The current fuel performance model has the same steady state irradiation creep component in tension and compression. The Standard ZIRLO™ data presented above show that steady state irradiation creep is the same for tension and compression hoop stresses. Therefore, the current fuel performance model assumption of similar steady state irradiation creep in tension and compression is consistent with the available Vogtle data.

#### 4.0 Summary

In compliance with Conditions 6 and 7 of Section 5.0 of the SER to topical report WCAP-12610-P-A & CENPD-404-P-A Addendum 1-A (Reference 1), the following information has been provided:

- Visual, oxidation of fuel rods, profilometry, fuel rod length, and fuel assembly length data for Optimized ZIRLO™ LTAs.
- Confirmation of the applicability of currently approved fuel performance models to Optimized ZIRLO™ based on available LTA data. Specifically, the model predictions of steady state creep are in agreement with profilometry measurements.
- Irradiation creep and irradiation growth data available from the Vogtle Creep/Growth tests.
- Confirmation of the applicability of currently approved fuel performance models to Optimized ZIRLO™ based on available Vogtle Creep/Growth data. Specifically, the irradiation creep of Standard ZIRLO™ is comparable to PRXA Optimized ZIRLO™, the stress dependence of the irradiation creep strain is linear, and steady state irradiation creep in tension and compression are the same for Westinghouse fuel cladding.

The Vogtle Creep/Growth measured data, LTA measured data, and favorable results from visual examinations of once-burned and twice-burned LTAs confirm, for at least two cycles of operation, that the current fuel performance models are applicable for Optimized ZIRLO™ fuel rods. Furthermore, since there is essentially no difference in the key performance parameters between Standard ZIRLO™ and Optimized ZIRLO™, it is expected that the existing fuel performance models will remain applicable for Optimized ZIRLO™ fuel rods to the licensed fuel burnup limit.

Additional data from the on-going Optimized ZIRLO™ LTA and Creep/Growth programs will be provided after new data for higher burnup/fluence become available.

#### 5.0 References

1. WCAP-12610-P-A & CENPD-404-P-A Addendum 1-A, "Optimized ZIRLO™," July 2006.
2. C. N. Tomé et al., "Role of Internal Stresses in the Transient of Irradiation Growth of Zircaloy-2," *Journal of Nuclear Materials*, Volume 227, 1996, pages 237-250.
3. M. McGrath, "In-reactor Creep Behavior of Zircaloy Cladding," International Topical Meeting on Light Water Reactor Fuel Performance, American Nuclear Society, Park City Utah, April 10-13, 2000.
4. J. Foster and M. McGrath, "In-Reactor Creep Behavior of Zircaloy Cladding," International Topical Meeting on Light Water Reactor Fuel Performance, American Nuclear Society, San Francisco CA, September 30-October 3, 2007.